GEOPHYSICS. VOL. 77, NO. 1 (JANUARY-FEBRUARY 2012); P. EN1–EN9, 6 FIGS.
10.1190/GEO2011-0160.1

Nonexponential decay of the surface-NMR signal and implications for water content estimation

Elliot Grunewald[1] and Rosemary Knight[1]

ABSTRACT

Noninvasive surface nuclear magnetic resonance (SNMR) measurements can yield direct and quantitative estimates of water content in the near surface. A fundamental assumption that is always made in the analysis of SNMR data is that the measured signal exhibits an exponential decay. Although the assumption of exponential decay is frequently valid, it can be shown that in the presence of an inhomogeneous magnetic field, the decay may be nonexponential in form. Simulated SNMR data were used to explore how the decay shape will vary with certain environmental and measurement conditions and to assess how nonexponential decay will affect SNMR-based estimates of water content. Results derived from analytical and pore-scale modeling demonstrated that the shape of the decay depends strongly on both pore geometry and the statistics of the regional or pore-scale magnetic field. In particular, the decay is most likely to be nonexponential when pores are large and when a strongly inhomogeneous magnetic field is present. For conditions in which the SNMR signal cannot be accurately modeled as exponential, standard processing approaches were found to result in significant errors in estimated water content — specifically, water content tends to be overestimated. Analysis of data misfits suggests that, in practice, it will be difficult to directly identify errors associated with nonexponential decay based only on the measured signal. Therefore, a description of the conditions leading to nonexponential decay and the implications for water content estimates is useful to support improved interpretation of SNMR measurements.

INTRODUCTION

Proton nuclear magnetic resonance (NMR) measurements provide direct sensitivity to the presence of hydrogen nuclei (protons) in pore fluids. NMR has been used for decades as a well-logging tool to determine formation properties including porosity, irreducible saturation, and permeability (Seevers, 1966, Timur, 1969, Kenyon et al., 1988). More recently, a surface-based NMR technique (SNMR) has been developed to probe the NMR response of groundwater aquifers (Legchenko and Valla, 2002; Hertrich, 2008; Walsh, 2008). The distinct advantage of SNMR over other surface-based geophysical techniques is that the recorded signal is emitted directly by groundwater and so can be used to quantify water content and potentially to obtain estimates of other hydrogeologic parameters. Achieving reliable interpretation of SNMR measurements, however, requires an accurate description of the physics controlling the measured signal. In this study, we investigate how the functional form of the SNMR signal can vary from a commonly assumed exponential decay and examine the impact of a nonexponential decay on estimates of water content.

In the standard SNMR measurement, large surface coils are used to excite hydrogen nuclei in groundwater and to measure their resonant free-induction decay (FID) response in the presence of Earth's magnetic field. The initial amplitude of the FID signal envelope E_0 can be directly related to the water content within the excited subsurface volume. Unfortunately, however, this initial amplitude is never directly measured due to a short instrumental recording delay known as the dead-time. Instead, water content is determined by extrapolating the recorded signal backward in time to estimate the initial amplitude.

A fundamental assumption that is always made when performing the extrapolation is that the FID exhibits an exponential or multiexponential decay. As such, an estimate of the initial amplitude $\hat{E}_0$ is derived using an exponential fit (Legchenko and Shushakov, 1998) or multiexponential fit (Mohnke and Yaramanci, 2005; Walsh, 2008; Mueller-Petke and Yaramanci, 2010) to the recorded signal. This

Manuscript received by the Editor 9 May 2011; revised manuscript received 9 September 2011; published online 3 February 2012.
[1]Stanford University, Department of Geophysics, Stanford, California, USA. E-mail: elliotg@stanford.edu; rknight@stanford.edu.

assumption is based on the fact that certain NMR decay processes, particularly those involved in NMR logging measurements, are indeed exponential in nature (Brownstein and Tarr, 1979). The FID signal, however, is influenced by an additional decay process, which arises in the presence of an inhomogeneous magnetic field; this process may result in signal decay that is nonexponential in form. The potential for nonexponential decay of the FID signal has been identified previously in the medical MRI literature (Sukstanskii and Yablonskiy, 2001) but not in the SNMR literature.

We hypothesize that if the SNMR FID deviates from an expected exponential form, the standard assumption of exponential decay will lead to significant errors in estimated water content. This basic concept is illustrated in Figure 1, where two theoretical FID signals are shown. The earliest-time portion of the two resonant signals, shown in gray, represents the dead-time when the signal cannot be recorded. The envelope $E(t)$ of the FID is shown as a thick black line with an initial amplitude E_0. In Figure 1a, the FID is accurately approximated as an exponential, and an exponential fit to the recorded signal (dashed gray line) yields an accurate estimate of the initial amplitude $\hat{E}_0$ (gray square). If instead the decay is nonexponential, as illustrated in Figure 1b, then fitting the signal as an exponential decay causes errors in the estimated value $\hat{E}_0$ and will result in subsequent errors in estimated water content.

The goal of this study is to identify the primary factors controlling the shape of the SNMR decay in geologic media and to quantify how this decay shape will affect estimates of water content. In our approach, we simulate and analyze synthetic SNMR signals representing a widely varied range of environment and measurement conditions. We first investigate synthetic SNMR signals generated using a simplified analytical model. This approach allows us to isolate the key parameters controlling the decay shape and to closely examine the potential magnitude of errors in water content under generalized conditions. We then simulate the FID signals directly using numerical pore-scale modeling in order to assess the potential influence of nonexponential decay errors in geologic materials. Our results demonstrate that nonexponential decay, though difficult to recognize in practice, can strongly influence the interpretation of SNMR data and diminish the accuracy of water content estimates. Given that conditions leading to nonexponential decay are likely to arise in the acquisition of SNMR field data, a better understanding of the signal decay shape can facilitate improved interpretation of SNMR data.

BACKGROUND AND THEORY

The SNMR method

The physics governing the SNMR measurement is similar to that governing borehole and laboratory NMR measurements. NMR measurements in geophysics probe the response of hydrogen nuclei in pore fluids to an excitation in the presence of a static background magnetic field. For borehole and laboratory NMR measurements, the static field $\mathbf{B}_0$ is generated by magnets or solenoids; for SNMR measurements, the static field is provided by Earth's natural geomagnetic field. At equilibrium with the static field, nuclear spins associated with the hydrogen nuclei preferentially align, giving rise to a net nuclear magnetization parallel to $\mathbf{B}_0$. The spins also precess about the static field at the Larmor frequency ω_0, given by

$$\omega_0 = -\gamma|\mathbf{B}_0|, \quad (1)$$

where γ is the gyromagnetic ratio of hydrogen ($0.2675\ \mathrm{rad} \cdot \mathrm{s}^{-1} \cdot \mathrm{nT}^{-1}$). The application of a secondary pulsed field $\mathbf{B}_1$, oscillating at the Larmor frequency and with a component perpendicular to $\mathbf{B}_0$, rotates a component of the magnetization into the plane transverse to $\mathbf{B}_0$. After the termination of this excitation pulse, continued precession of the magnetization in the transverse plane generates a detectable signal, which resonates at the Larmor frequency and decays over time as the spins relax to equilibrium.

For the SNMR measurement, acquired in Earth's field, one or more large surface coils are used to transmit the excitation pulse and to subsequently record the NMR response from groundwater at depth. The excitation pulse is generated by passing an alternating current I (typically up to 600 A) tuned to the Larmor frequency (1.3–2.6 kHz depending on geographic location) through the coil for a specific duration τ_{pulse}. By varying the excitation pulse moment q, given by the product $I \cdot \tau_{\mathrm{pulse}}$, volumes of groundwater at different depths are investigated, and a spatial inversion is used to resolve the NMR response as a function of depth.

The NMR response following a single excitation pulse is referred to as the free induction decay and can be most generally expressed as

$$FID(t) = E(t)e^{i\omega_0 t} = E(t) = e^{i\gamma|B_0|t}, \quad (2)$$

where the decay envelope $E(t)$ is related to the abundance and physical environment of the excited spins. Of central importance for groundwater investigations is the fact that the initial amplitude of the envelope E_0 directly reflects the volume of water excited by the surface coil.

Unfortunately, it is not possible to directly measure E_0, due to a short recording delay known as the dead-time τ_{dead}, typically between 4 and 40 ms (Walsh et al., 2009). Instead, the decay envelope is extrapolated back to time-zero based on the signal measured after the dead-time. Time-zero is typically referenced to the end of the excitation pulse, but may alternatively be referenced to the middle of the pulse (Walbrecker, et al., 2009) to compensate for decay during the pulse.

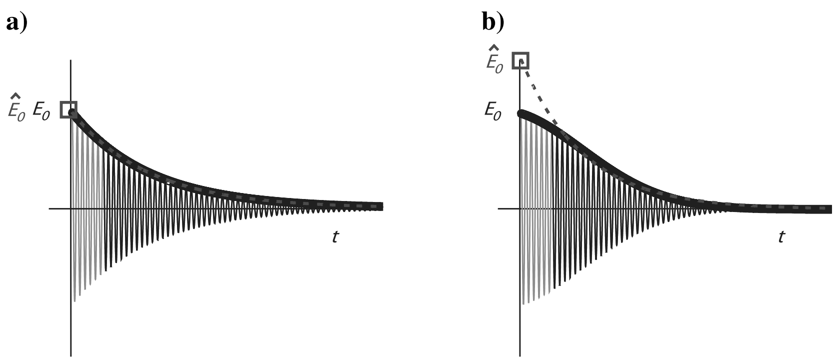

Figure 1. Schematic illustrations of the resonant FID signal exhibiting (a) exponential and (b) nonexponential decay. The portion of the signal in gray occurs during the dead-time and is not recorded. The thick black line shows the decay envelope $E(t)$ with initial amplitude E_0. A gray box reflects the estimated value $\hat{E}_0$ derived from an exponential fit (dashed) to the recorded data.

Various inversion schemes implement this extrapolation step in a slightly different manner: extrapolating the measured FIDs prior to a spatial inversion (Legchenko and Shushakov, 1998), extrapolating the measured FIDs concurrent with a spatial inversion (Mueller-Petke and Yaramanci, 2010), or extrapolating spatially resolved FIDs following an initial spatial inversion step (Walsh, 2008). What is common to all of these approaches, though, is a fundamental assumption that $E(t)$ follows an exponential or multiexponential decay. Following this assumption, estimates of $\hat{E}_0$ and water content are always derived using an exponential or multiexponential fit to the recorded data. The extent to which this important assumption is valid, however, depends upon variable factors related to the pore-scale physical environment.

The SNMR decay shape

The decay envelope of the FID reflects the combined influence of three simultaneously occurring decay processes: bulk-fluid relaxation, surface-relaxation, and inhomogeneous dephasing. Although the first two decay processes are exponential in character, the third can be nonexponential in character. It is the relative magnitude of the decay times associated with each of these processes that ultimately determines the decay behavior of the FID signal.

Both bulk-fluid relaxation and surface-relaxation occur as exponential decay processes. Bulk-fluid relaxation arises due to molecular-scale interactions between spins in the fluid and with dissolved paramagnetic ions (Bloembergen et al., 1948). Surface relaxation arises as diffusing spins encounter the grain surface and interact with paramagnetic sites on the pore wall. In the hypothetical case of a uniform background magnetic field, bulk-fluid and surface-relaxation are the only processes contributing to the decay of the FID signal in a porous medium. In this hypothetical condition, the decay envelope of the FID arising from water in a homogeneous aquifer can be written as an exponentially decaying function:

$$E(t)_{\text{uniform}} = E_0 e^{-t/T_{2B}} e^{-t/T_{2S}}, \tag{3}$$

where the subscript "uniform" denotes the assumption of a uniform background field, T_{2B} is the bulk-fluid relaxation time and T_{2S} is the surface relaxation time. The bulk-fluid relaxation time for water is typically between 1 and 3 seconds and depends only on the properties of the pore fluid.

The surface relaxation time is typically much shorter than the bulk-fluid relaxation time and reflects the geometric and geochemical properties of the pore space. For the condition of fast diffusion (Brownstein and Tarr, 1979), requiring that diffusion to the grain surface is not the rate limiting process, the surface relaxation time is given by the expression:

$$\frac{1}{T_{2S}} = \rho_2 S/V \tag{4}$$

where S/V is the surface-area-to-volume ratio of the pore space (inversely proportional to the pore radius for simple pore geometries), and ρ_2 is the surface relaxivity, a property describing the capacity of the grain surface to enhance relaxation. This fast-diffusion regime, in which T_{2S} exhibits a linear trend with pore size, is valid in many geologic materials. In materials with very large pores (e.g., coarse sands) or with high surface relaxivity (e.g., due to iron alteration), diffusion to the pore surface can be the rate-limiting process; in the slow-diffusion regime that governs such cases, T_{2S} exhibits a quadratic rather than linear increase with pore size. In either regime, surface relaxation typically dominates the decay signal measured by NMR logging instruments and is the basis for the sensitivity of NMR measurement to pore size and permeability. In rocks with a distribution of pore sizes, a multiexponential decay is frequently observed; water in small pores contributes signal components with short T_{2S} and water in large pores contributes components with long T_{2S}.

For simplicity, we will consider signals exhibiting single-exponential decay and combine the bulk-fluid and surface-relaxation terms to rewrite equation 3 as

$$E(t)_{\text{uniform}} = E_0 e^{-t/T_{2BS}}, \tag{5}$$

where $1/T_{2\text{BS}} = 1/T_{2\text{B}} + 1/T_{2\text{S}}$, representing the combined effect of both relaxation mechanisms in the presence of a uniform background magnetic field.

In natural geologic environments, the background field is never perfectly uniform and spatial field variation gives rise to an additional decay process, inhomogeneous dephasing, that can be nonexponential in character. Laboratory and logging NMR measurements utilize pulse sequencing to measure signals in which inhomogeneous dephasing effects are effectively reduced or eliminated, but the FID signal measured by SNMR is always influenced by dephasing. A spatially inhomogeneous magnetic field $\mathbf{H}(\mathbf{r})$ superimposed on $\mathbf{B}_0$ can arise at the pore scale due to the presence of magnetic grains, or at the field scale due to local magnetic anomalies. In the presence of a spatially variable field, spins at different positions $\mathbf{r}$ experience a different total background field, and thus resonate at slightly different Larmor frequencies (equation 1). As a result, the resonant signal dephases over time, leading to a decay which we represent by the inhomogeneous dephasing function $h(t)$. Generally, inhomogeneous dephasing can be considered as processes independent from bulk- and surface-relaxation, and the FID envelope can be expressed as

$$E(t) = E_0 e^{-t/T_{2BS}} h(t). \tag{6}$$

In all previous SNMR studies a simplifying assumption is made that $E(t)$ can be described as a basic exponential (or multiexponential) decay written as

$$E(t) = E_0 e^{-t/T_2^*}, \tag{7}$$

where the effective decay time T_2^* is intended to represent the combined contribution of bulk-fluid relaxation, surface relaxation, and dephasing. Modeling the FID envelope in this way, however, implicitly assumes that inhomogeneous dephasing can be neglected or that the dephasing function $h(t)$ can be accurately approximated as an exponential decay with a characteristic inhomogeneous dephasing decay time T_{2IH}, such that $1/T_2^* = 1/T_{2BS} + 1/T_{2IH}$. This simplification, however, is not necessarily appropriate: decay due to inhomogeneous dephasing is rarely negligible and will not necessarily be exponential in form.

A more precise description of the dephasing function $h(t)$ can be obtained by considering the actual signal arising from an ensemble of spins resonating at different frequencies in an inhomogeneous field. We can describe an inhomogeneous field as the superposition of a primary background field $\mathbf{B}_0$ and a zero-mean, spatially variable field $H(\mathbf{r})$. According to equation 1, the resonant frequency of the spins at a given position $\mathbf{r}$ in the inhomogeneous field, is given by $\gamma[|\mathbf{B}_0| + H(\mathbf{r})]$, where $H(\mathbf{r})$ is the component of the inhomogeneous secondary field that is parallel to $\mathbf{B}_0$. If we briefly ignore relaxation and diffusion, the net resonant signal $h_r(t)$ from an ensemble of spins resonating in an inhomogeneous field can thus be expressed by the integral,

$$h_r(t) = \int_{-\infty}^{+\infty} P[H] e^{i\gamma(|B_0|+H)t} \mathrm{d}H, \tag{8}$$

where $P[H]$ is the probability distribution of the secondary inhomogeneous field over the volume of excited spins. Reducing equation 8 to baseband and recognizing the Fourier transform relationship we can more simply express the envelope of the dephasing function as

$$h(t) = e^{i\gamma B_0 t} h_r(t) = \frac{1}{\gamma} F\{P[H]\}. \tag{9}$$

This Fourier transform relationship, which has been described previously in the medical MRI literature (e.g., Sukstanskii and Yablonskiy, 2001), precisely determines both the shape and decay rate of the dephasing function $h(t)$ for the static case when diffusion of spins can be neglected. The relationship remains approximately valid as long as the scale over which the inhomogeneous field varies is not much smaller than the distance a spin can sample by diffusion before dephasing.

In Figure 2 we illustrate how the shape of $h(t)$ will vary for three hypothetical magnetic-field distributions: (a) Lorentzian, (b) Gaussian, and (c) rectangular. We see that only for the case of a Lorentzian distributed field is $h(t)$ exponential in form. If $P[H]$ is Gaussian, $h(t)$ will also be Gaussian; if $P[H]$ is rectangular $h(t)$ will be a sinc function. We note that for both the Gaussian and rectangular distributions, $h(t)$ exhibits a steep slope like an exponential at intermediate times, but is rounded at early times. This characteristic is a consequence of the fact that sharp features in the time-domain require high frequencies in the Fourier-domain; the specific sharp feature of an exponential decay at early times requires the longer tails contained in the Lorentzian distribution.

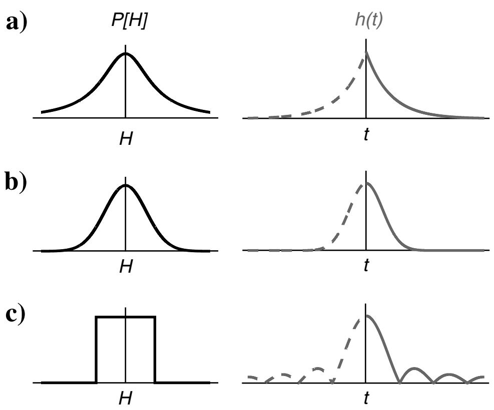

Figure 2. Examples illustrating the dephasing decay function $h(t)$, shown in gray, corresponding to three different inhomogeneous magnetic field distributions $P[H]$, shown in black: $P[H]$ is (a) Lorentzian, (b) Gaussian, and (c) rectangular.

The Fourier transform relationship also determines the rate at which $h(t)$ decays. A function that is wide in the Fourier domain is narrow in the time domain. Thus, if we define T_{2IH} as the characteristic time for $h(t)$ to decay to a factor of $1/e$ (i.e., $h(T_{2IH}) = h(0)/e$), T_{2IH} will become shorter as $P[H]$ becomes broader (i.e., as the second moment of $P[H]$ increases with greater variation in the magnetic field).

Combining equations 6 and 9 into a single expression for the decay envelope,

$$E(t) = E_0 \frac{1}{\gamma} F\{P[H]\} e^{-t/T_{2BS}}, \tag{10}$$

we see that the shape of the FID ultimately depends on the magnetic field distribution as well as the relative magnitude of the characteristic decay times T_{2BS} and T_{2IH}. If T_{2IH} is much longer than T_{2BS} ($T_{2BS}/T_{2IH} \ll 1$), the exponential relaxation term will dominate and the resulting FID envelope will be exponential. If, on the other hand, T_{2IH} is much shorter than T_2 ($T_{2BS}/T_{2IH} \gg 1$), inhomogeneous dephasing will dominate, and the FID will primarily reflect the shape of $h(t)$, which may be nonexponential. Thus the FID shape is sensitive both to pore-scale properties, through T_{2BS}, as well as the properties of the inhomogeneous magnetic field. Because both of these properties vary naturally in the environment, we must examine how the decay shape and estimates of water content can be expected to vary across a range of conditions.

SYNTHETIC SNMR DATA

We generate and analyze synthetic SNMR decay signals, designed to represent a broadly varied range of environmental and measurement conditions, using two complementary approaches. In our first approach, we utilize a simple analytical model that allows us to isolate the key parameters controlling the decay shape and to characterize the errors associated with nonexponential decay arising in the presence of a generalized inhomogeneous magnetic field. In the second set, we conduct direct pore-scale simulation of the FID signal in magnetic porous media to assess the importance of nonexponential decay given accurate pore-scale physics and realistic measurement conditions.

Analytical modeling

In our first approach, we generate a suite of synthetic FID signals using a simple analytical model that treats relaxation and dephasing as scale-independent processes and neglects diffusion. Given these assumptions and specifying hypothetical values for the parameters T_{2BS} and $P[H]$, we simulate the resulting decay envelope $E(t)$ based on equation 10. Between simulations, we vary T_{2BS} and $P[H]$ to explore a wide range of conditions in which the SNMR decay may be influenced by the properties of the physical environment.

We explore three different magnetic field distributions $P[H]$ corresponding to the three examples illustrated previously in Figure 2. A Lorentzian distribution approximately describes the anomaly field arising from randomly distributed magnetic dipoles (Brown, 1961). A Gaussian or rectangular distribution, on the other hand, is generally appropriate to model the anomaly field within a homogeneous magnetic sediment (Audoly et al., 2003). A rectangular distribution can be used to describe the anomaly from a magnetic body located at a sufficient distance that the field varies linearly. For each of these three $P[H]$ cases, we calculate the corresponding FID envelope according to equation 10. Between simulations, we also vary the value of T_{2BS} to create a suite of signals between which the ratio T_{2BS}/T_{2IH} varies over four decades; in this ratio, T_{2IH} is defined as $h(T_{2IH}) = 1/e$ for a generalized dephasing function.

Given the simulated signals, we directly assess the potential for errors in estimated water content by processing each synthetic $E(t)$ signal as though it were an actual SNMR measurement. For a given instrument dead-time τ_{dead}, we first clip the early-time portion of the decay that would not be recorded; we also add 5% random noise to the signal. Following the standard assumption of exponential decay, we then use a least-squares fit of equation 7 to the data to determine estimated values $\hat{T}_2^*$ and $\hat{E}_0$. As is recommended practice in SNMR processing, we specify a lower bound on the fitted value of $\hat{T}_2^*$ equal to τ_{dead} to avoid spurious fitting of short signals that cannot be adequately resolved. We execute this fitting process for each synthetic decay and repeat the fitting process using varied values of τ_{dead}, such that the ratio $\tau_{\mathrm{dead}}/T_2^*$ varies between 0 and 1, where T_2^* is approximated as $1/T_2^* = 1/T_2 + 1/T_{2IH}$.

In Figure 3, we display simulation results in three separate color plots corresponding to the three cases where $P[H]$ is (a) Lorentzian, (b) Gaussian, and (c) rectangular. The color at each position indicates the relative error in water content, $\varepsilon = \hat{E}_0/E_0$, for each simulation with the corresponding simulation parameters shown on the two axes. On the horizontal, logarithmic axis we plot the ratio T_{2BS}/T_{2IH}, identified above as a key parameter governing the decay shape. On the vertical axis, we plot the ratio $\tau_{\mathrm{dead}}/T_2^*$, representing the fraction of the signal that decays during the dead-time. Warm colors indicate overestimated water content ($\varepsilon > 1$); blue indicates underestimated water content ($\varepsilon < 1$); gray indicates an accurate estimate ($\varepsilon \sim 1$).

We first consider the case of a Lorentzian distribution, shown in Figure 3a. In this case, water content errors are negligible for all simulations; i.e., $\varepsilon \sim 1$ (gray) for all simulations. This is because the corresponding dephasing function $h(t)$ for a Lorentzian distributed field is precisely an exponential decay. Thus, in this specific case, the decay envelope $E(t)$ will always be exponential, regardless of the relative magnitude of T_{2BS} and T_{2IH}. As a result, an exponential fit to the recorded signal will always yield an accurate estimate of E_0 (as shown in Figure 1a).

The situation changes and errors are more significant when the magnetic field distribution is no longer Lorentzian. For the case of a Gaussian distributed field, shown in Figure 3b, the corresponding dephasing function $h(t)$ is no longer exponential, but is instead Gaussian. In this case, we find that errors are only negligible when the ratio T_{2BS}/T_{2IH} is small (left side of plot). When $T_{2BS}/T_{2IH} \ll 1$, the exponential term T_{2BS}-term dominates and $E(t)$ can be reasonably approximated as an exponential even though $h(t)$ is not exponential. As we cross into the regime of $T_{2BS}/T_{2IH} \gg 1$ (right side of plot), however, E_0 becomes significantly overestimated. These errors occur because as T_{2BS}/T_{2IH} increases, dephasing begins to dominate and the expression for $E(t)$ more strongly reflects the nonexponential shape of $h(t)$. In this case, the exponential fit is biased by the steep slope of the Gaussian function at intermediate times, and when extrapolated backward in time, the initial envelope amplitude is overestimated.

When the dead-time is very short relative to the decay time (lower edge of plot), water content is only moderately overestimated ($\varepsilon \sim 1.2$). As $\tau_{\mathrm{dead}}/T_2^*$ increases, however, the error becomes increasingly severe until a maximum at $\tau_{\mathrm{dead}}/T_2^* \sim 0.5$, where E_0 is overestimated by more than a factor of two. This dependence on the dead-time reflects the fact that the exponential fit is more strongly biased by the steep slope of $h(t)$ at intermediate times when the shallowly sloping portion of the decay at early-time is not recorded. We note that as $\tau_{\mathrm{dead}}/T_2^*$ approaches unity, water content eventually becomes underestimated. This underestimation occurs because the signal at late times has decayed to a value lower than that which can be modeled by an exponential decay given a restricted lower bound of $\hat{T}_2^* = \tau_{\mathrm{dead}}$. We note that if the estimated value of $\hat{T}_2^*$ is not constrained by this lower bound, overestimation of E_0 will continue to increase with $\tau_{\mathrm{dead}}/\hat{T}_2^*$ (eventually by more than a factor of five for $\tau_{\mathrm{dead}}/T_2^* = 1$).

For the rectangular distributed field, shown in Figure 3c, we find very similar results to the Gaussian case, though the magnitude of errors in water content are somewhat larger. This overall similarity can be attributed to the fact that the corresponding sinc-shaped dephasing function, like a Gaussian function, exhibits a shallow slope at early-time and a much steeper slope at intermediate-time. Thus, the initial amplitude is overestimated, especially when the shallow sloping portion of the signal at early-time is not recorded. Again, when the dead-time is long, the signal is too small to be modeled by an exponential, given the lower bound on the estimated value of $\hat{T}_2^*$, and we observe underestimation of E_0 for large values of $\tau_{\mathrm{dead}}/T_2^*$.

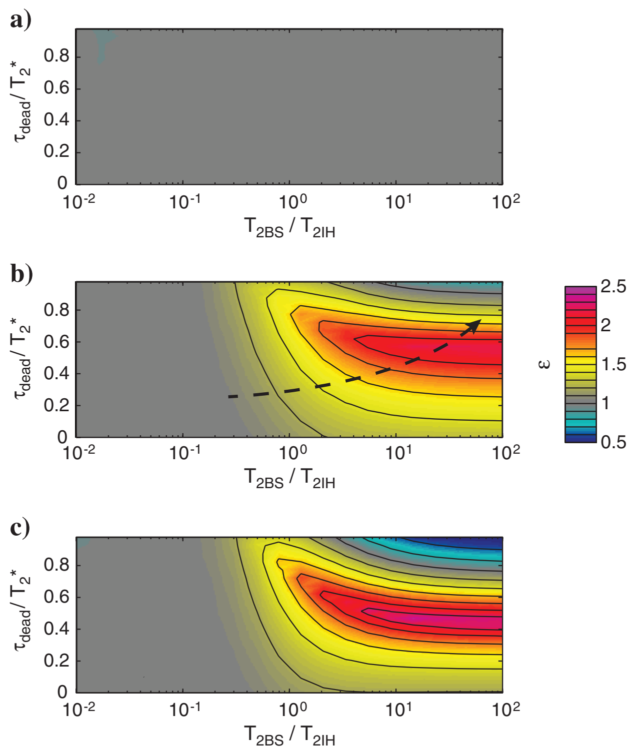

Figure 3. Color plots illustrating the relative error ε in water content resulting from an exponential fit to synthetic FID envelopes. The relative error is calculated as the estimated value of E_0 normalized by the true value. Parameters describing each simulation are shown on the horizontal and vertical axes. Between the three panels, the distribution $P[H]$ varies: (a) Lorentzian, (b) Gaussian, and (c) rectangular. The trajectory indicated by the dashed black line in (b) represents the trend associated with increasing pore size or magnetic inhomogeneity.

The units for the axes in Figure 3 have been made dimensionless so that these simulation results can be generalized to describe a wide range of measurement conditions. We can also use these results to examine and quantify the influence of nonexponential decay for a particular set of conditions. Referring back to Figure 1b, this particular decay envelope was actually simulated analytically assuming a Gaussian distribution for $P[H]$, $T_{2BS}/T_{2IH} = 2.0$ and $\tau_{\mathrm{dead}}/T_2^* = 0.45$. Given a relatively long instrument dead-time of 30 ms, these ratios correspond to realistic values of $T_{2IH} =$ 100 ms and $T_{2BS} = 200$ ms. For this example, we see that the exponential fit (dashed line) is strongly biased by the steeper slope of the decay at intermediate times and E_0 is overestimated by 60%.

Upon closer examination of the exponential fit in this example, we note that even though E_0 is significantly overestimated, the exponential approximation appears to provide a reasonable fit to the truncated portion of the signal recorded after the dead-time. The apparent strength of the fit to the recorded signal has an important practical consequence. It implies that the nonexponential character of the decay at early times is likely to be obscured by the dead-time and thus may not be easily recognized as a problem in practice.

To more closely explore this issue, we investigate the data residuals from the exponential fits to the previously simulated FID signals. In Figure 4, we show results for the synthetic signals corresponding to the case of a Gaussian distributed field. On the same axes as previously, the color of the plot now reflects value of the normalized data residual determined from the exponential fit to the synthetic decay. The normalized residual is calculated as

$$\frac{\|d_{pred} - d_{\mathrm{obs}}\|}{\sqrt{\sigma}}, \tag{11}$$

where d_{pred} is the predicted signal from the exponential fit, d_{obs} is the synthetic signal, and σ is the variance of the synthetic noise. Larger values of the normalized residual indicate a poorer fit; a value of one indicates a statistically perfect fit.

As can be expected, the exponential model provides a good fit when the condition $T_{2BS}/T_{2IH} \ll 1$ is satisfied and the decay is truly exponential. However, we also observe a good apparent fit in certain cases when T_{2BS}/T_{2IH} is large and the decay is nonexponential. In particular, the residual remains especially small for simulations in which $\tau_{\mathrm{dead}}/T_2^*$ is intermediate-valued. We note that under these same conditions in which the exponential model yields a good apparent fit to the data, we also find the most problematic errors in water content. In such cases, the most nonexponential portion of the decay at early times is truncated, yielding a better fit to the recorded data and a stronger biasing of the steeper slope at intermediate times. Thus, errors associated with nonexponential decay are unlikely to be directly apparent from the observed shape of the recorded SNMR signal, even under conditions in which these errors are especially problematic.

Here we have considered cases where dephasing occurs as a nonexponential decay, and surface relaxation occurs as a single exponential decay. In many geologic materials, surface relaxation can also occur as a multiexponential decay, either because there is an underlying distribution of pore sizes, or because multiple relaxation modes are observed in the slow diffusion regime. We predict that the occurrence of multiexponential surface relaxation will further tend to obscure the identification of nonexponential behavior affecting the FID signal.

We illustrate this hypothesis in Figure 5, where we show a synthetic FID signal modeled according to equation 6, but modified to include two exponential relaxation-time components as follows:

$$E(t) = h(t)\left(A_{\mathrm{long}} e^{-t/T_{2BS,\mathrm{long}}} + A_{\mathrm{short}} e^{-t/T_{2BS,\mathrm{short}}}\right). \tag{12}$$

Here A_{long} is the fractional signal component exhibiting a long relaxation-time $T_{2BS,\,long}$ (e.g., the fraction of water in large pores) and the subscript "short" denotes a signal component with a short relaxation-time (e.g., in small pores). In the case that $T_{2BS,\,short}/T_{2IH} \ll 1 \ll T_{2BS,\mathrm{long}}/T_{2IH}$, the long-time component of the signal (thin black line) will reflect the nonexponential character reflecting the case of the dephasing function (in this case Gaussian), while the short-time component (thin gray line) will exhibit a short exponential decay. Adding the short-time component to the long-time component (gray shading) yields the net FID signal (thick black line).

We see that this FID signal with two exponential relaxation terms is actually well approximated by a single exponential fit (red line), even if dead-time (dashed region) is relatively short. While the fit appears to be good, it actually misrepresents the underlying relaxation behavior. Specifically, because the net FID appears to follow a single, long-time exponential decay, one would tend to overestimate the fraction of water associated with long decay times (i.e., in large

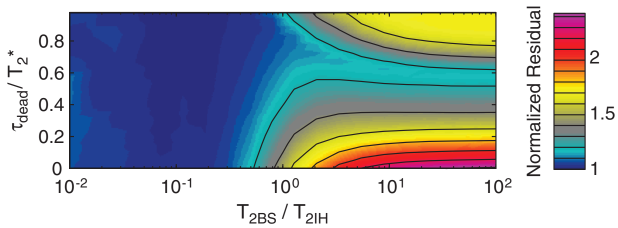

Figure 4. Color plots illustrating the normalized residual resulting from the exponential fit to each synthetic FID envelope. The normalized residual is calculated as the total residual normalized by the expected value of the residual, given the noise level; larger values indicate a poorer fit; a value of one indicates a statistically perfect fit. Parameters describing each simulation are shown on the horizontal and vertical axes. The inhomogeneous field distribution $P[H]$ is Gaussian (corresponding to panel (b) in Figure 3).

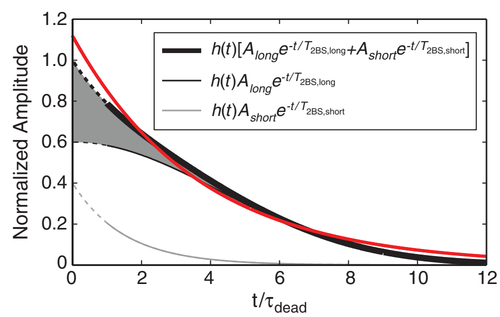

Figure 5. Synthetic signals modeling an FID with two relaxation-time components. The components with long and short relaxation times are shown as thin black and gray lines, respectively. Summing these two components yields the net FID decay envelope (thick black line). The red line shows the fit on an exponential function to the FID envelope, given a finite dead-time indicated by the dashed lines.

pores), and would fail to identify the presence of signals with short relaxation times. Thus, the properties of the subsurface would not be accurately characterized. It should be noted that fitting the FID with a multiexponential function cannot be expected to resolve this problem. A multiexponential function, which steepens more sharply than a single-exponential function at early times, will only tend to further overestimate water content when the signal contains a nonexponential decay component.

Pore-scale numerical modeling

The previous set of simulations illustrates how basic parameters describing relaxation (T_{BS}) and inhomogeneous field dephasing ($P[H]$) will affect the decay shape and estimates of water content under a wide range of generalized conditions. In practice, these parameters and the resulting shape of the SNMR decay will vary as a function of the local geologic environment and physics operating at the pore scale. Specifically, bulk-fluid and surface-relaxation will be controlled by geometric and mineralogical properties of the aquifer material, while dephasing will be controlled by the presence of magnetic geology. To directly assess how the decay shape and estimates of water content will vary in specific aquifer materials, we conduct direct pore-scale simulations of the SNMR signal.

We simulate the FID response for water in homogeneous sediment using a 1D pore model and random-walk algorithm developed by Grunewald and Knight (2011). The pore model has a radius r and is bounded on either side by a grain with surface relaxivity ρ_g and magnetic susceptibility χ_g. Across the pore, a spatially variable internal magnetic field $H(x)$ arises as a function of the magnetic susceptibility of the grain. The magnitude and statistics of the internal field are calculated after Audoly et al. (2003) who directly simulate the magnetic field arising from a dense random pack of magnetic spheres. The distribution $P[H]$ of this field across the pore is approximately Gaussian, zero-mean, and has a second moment that is proportional to the product of the grain susceptibility and the background field B_0. For a given parameterized pore model we simulate the complete FID signal using a random-walk algorithm, described in Grunewald and Knight (2011). In contrast to the previous analytical models which neglect diffusion and treat relaxation and dephasing as a scale-independent parameters, the random walk algorithm fully incorporates molecular diffusion and directly simulates surface relaxation and inhomogeneous dephasing as pore-scale processes.

We compile a suite of pore-scale simulations between which we vary the model parameters to be representative of a wide range of geologic media. We logarithmically vary the pore radius from 5 to 500 μm and susceptibility from 20 to 2000×10^{-6} cgs; we fix surface relaxivity at an intermediate value of 20 μm/s. Given surface relativity and the range of pore size, our simulations include relaxation in both the fast- and slow-diffusion regimes; for all simulations B_0 is fixed at 50,000 nT, a representative value for Earth's field at mid-latitudes. As in the previous section, we treat each simulated signal as an actual SNMR signal. We add 5% Gaussian noise and truncate the early-time portion of the signal to simulate the dead-time. To determine the value of E_0 that would be estimated under the standard assumption of exponential decay, we again use a least-squares fit of equation 7 to the signal envelope.

In Figure 6, we plot the resulting relative error ε in the estimated value $\hat{E}_0/E_0$ versus the ratio T_{2BS}/T_{2IH} for the suite of simulations assuming a dead-time of (6a) 30 ms and (6b) 10 ms. Each point corresponds to a single simulation result; the size of the point reflects the pore radius (the smallest point corresponds to a radius of 5 μm — the largest point corresponds to a radius of 500 μm); the color of the point reflects the grain susceptibility (blue roughly corresponds to the susceptibility of quartz or feldspar, red roughly corresponds to hematite).

We find that errors are negligible when the susceptibility is low and for moderate susceptibility when the pore size is small. When susceptibility is low, the magnetic field is weak and T_{2IH} is long; when the pore size is small, surface relaxation is rapid and T_{2BS} is very short. In either case, the condition $T_{2BS}/T_{2IH} \ll 1$ is satisfied, and the decay is accurately approximated as an exponential. As pore size or susceptibility increases, however, errors become more significant. Increasing pore size increases T_{2BS} in the numerator because spins undergo surface relaxation more slowly in large pores. Increasing susceptibility decreases T_{2IH} in the denominator because dephasing is more rapid when the internal magnetic field is

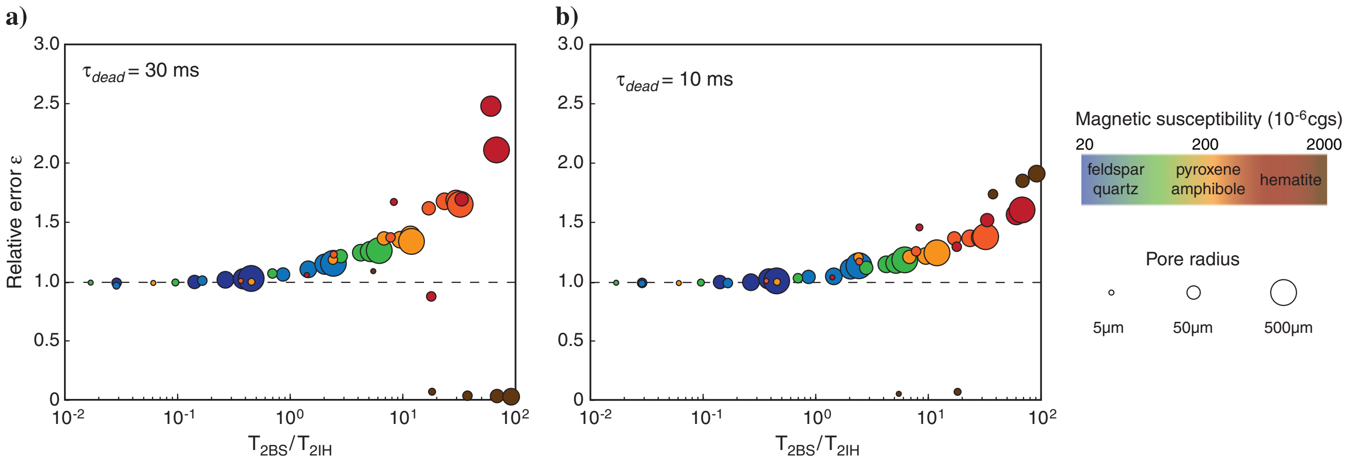

Figure 6. Relative error ε in water content resulting from an exponential fit to synthetic FID envelopes generated from pore-scale simulations given a dead-time of (a) 30 ms and (b) 10 ms. The relative error is calculated as the estimated value of $\hat{E}_0$ normalized by the true value. Each point represents one simulation result; magnetic susceptibility is indicated in warming colors; pore size is indicated by the size of the point. The horizontal axis reflects the parameter T_{2BS}/T_{2IH}, related to the decay shape.

stronger and exhibits a higher variance. Because the internal field is approximately Gaussian, as the value of T_{2BS}/T_{2IH} increases, the decay becomes increasingly nonexponential and exhibits a shallow slope at early times. As seen previously, under these conditions the exponential fit is biased by the steeper slope of the decay at intermediate times and water content is overestimated.

Our simulation results further allow us to predict the potential magnitude of water content estimation errors under a range of realistic survey conditions. Considering a dead-time of 30 ms, we find that for a sand of intermediate susceptibility, E_0 may be overestimated by around 10% to 30%. For higher susceptibility sediments, this error increases and water content may eventually be overestimated by more than a factor of two. We note that as susceptibility becomes very high (brown points), the signal entirely decays within the span of the dead-time and water content is grossly underestimated. In the context of our previous results based on an analytical model, this trend with pore size and susceptibility can be viewed as a diagonal trajectory across Figure 3b from the bottom-left to the top-right. When the dead-time is reduced from 30 to 10 ms, water content errors are significantly reduced but are still large when magnetic susceptibility is high. Recent advancements in SNMR hardware have achieved instrument dead-times as short as 4 ms (Walsh et al., 2011). The influence of decreasing the dead-time can be viewed as a downward shift of the previously described diagonal trajectory across Figure 3, leading to a reduction in water content estimation errors.

These pore-scale simulations model the response of homogeneous sediments in which the internal field is approximately Gaussian. For heterogeneous sediment containing sparsely dispersed, magnetic grains, the pore-scale internal magnetic field distribution will be more closely Lorentzian in form (Brown, 1961). Thus, in heterogeneous sediments, nonexponential decay errors are likely to be less severe and may not show the same dependence on the magnetic susceptibility of the grains. On the other hand, if the inhomogeneous field arises due to larger scale features (e.g., a magnetic intrusion), the decay shape will be dependent on the statistics and geometry of the specific magnetic anomaly and be nonexponential, even if the aquifer sediments themselves are weakly magnetic.

In both of our approaches to the simulation of SNMR data, we have assumed that inhomogeneity in the magnetic field only influences the decay of the SNMR signal and not the excitation of the nuclear spins. This assumption is valid given that the variance in resonant frequencies (proportional to the variance in the magnetic field) is smaller than the bandwidth of the excitation pulse. This condition will be satisfied given moderate field inhomogeneity and short excitation pulses. We note that for extreme conditions in which the variance in resonant frequencies becomes much larger than the bandwidth of the excitation pulse, only a portion of the spins will be excited and the decay shape will be primarily determined by the spectrum of the transmitted excitation pulse; in such cases, we anticipate even larger errors in water content.

CONCLUSIONS

This study investigates the validity of a simple assumption that the FID signal measured by SNMR can be modeled as an exponential decay. By generating and analyzing synthetic SNMR data, we demonstrate that under realistic geologic conditions, the decay can commonly be nonexponential in form. The shape of the decay depends both on pore geometry and on the character of the regional or pore-scale magnetic field. Specifically, we find that the decay is likely to be nonexponential when pores are large and when the background magnetic field is strongly inhomogeneous . Such conditions are most likely to occur near regional magnetic anomalies or in the presence of magnetic sediments (e.g., those containing magnetite, hematite, or maghemite). For cases in which the SNMR signal is not accurately modeled as exponential, we show that standard processing approaches can lead to significant errors and generally result in overestimation of water content.

In addition to illustrating the manner in which environmental conditions affect the decay shape, we also demonstrate the critical importance of the duration of the instrument dead-time relative to the effective decay time. We show that nonexponential decay is likely to be more problematic if the dead-time is long. A long dead-time not only increases the potential for errors in estimated water content, but can also mask the nonexponential character of the decay such that these errors are unlikely to be readily noticed in practice.

One approach to directly assessing and mitigating the potential problems associated with nonexponential decay is to utilize SNMR instrumentation with a short dead-time. We have shown, however, that the character of the decay may still be obscured by the occurrence of multiexponential surface relaxation. The presence of noise will also limit the extent to which the decay shape can be directly characterized. Here we have assumed a conservative estimate of 5% Gaussian noise for the numerical simulations; in practice, SNMR data may be subject to noise ranging from less than a few percent to more than 100%.

Other approaches implemented during inversion and interpretation might be devised to partly account for a variable decay shape. For example, a conservative lower bound on water content might be estimated by fitting the decay envelope as a Gaussian, while an upper bound may be estimated by fitting the decay as an exponential. A single function containing a product of an exponential term and a Gaussian term might also be used. Alternatively, it might be possible to explicitly characterize the decay shape on a site-by-site basis using measurements of the magnetic field variation or SNMR measurements of spin echoes. Neglecting diffusion, the shape of the spin echo signal should symmetrically reflect the shape of the FID and so might be used to more appropriately model the shape of the FID at early times.

This study presents theoretical predictions regarding the impact of nonexponential decay on SNMR measurements. In future research, it will be important to identify and characterize the practical prevalence and implications of nonexponential decay in actual SNMR field data. It will also be helpful to utilize laboratory experiments in which very short dead-time can be achieved and measurement conditions can be closely controlled. Further research on this topic will not only improve our understanding of the SNMR signal, but will also allow us to develop more robust approaches to processing and interpreting these informative measurements.

ACKNOWLEDGMENTS

This research was supported by funding to R. Knight from the National Science Foundation, award EAR-0911234. Further support for E. Grunewald was provided by a scholarship from the Society of Exploration Geophysicists Foundation. We thank Y.-Q. Song for providing calculations of the internal magnetic field used for the pore-scale simulations.

REFERENCES

Audoly, B., P. N. Sen, S. Ryu, and Y.-Q. Song, 2003, Correlation functions for inhomogeneous magnetic field in random media with application to a dense random pack of spheres: Journal of Magnetic Resonance, **164**, 154–159, doi: 10.1016/S1090-7807(03)00179-4.

Bloembergen, N., E. M. Purcell, and R. V. Pound, 1948, Relaxation effects in nuclear magnetic resonance absorption: Physical Review, **73**, 679–712, doi: 10.1103/PhysRev.73.679.

Brown, R. J. S., 1961, Distribution of fields from randomly placed dipoles: Free-precession signal decay as result of magnetic grains: Physical Review, **121**, 1379–1382.

Brownstein, K. R., and C. E. Tarr, 1979, Importance of classical diffusion in NMR studies of water in biological cells: Physical Review A, **19**, 2446–2453.

Grunewald, E., and R. Knight, 2010, Conditions leading to non-exponential decay of the surface-NMR signal and implications for water content estimation, 79th Annual International Meeting, SEG, Expanded Abstracts, **29**, 3951–3955 doi: 10.1190/1.3513675.

Grunewald, E., and R. Knight, 2011, The effect of pore size and magnetic susceptibility on the surface NMR relaxation parameter T_2^*: Near Surface Geophysics, **9**, 169–178.

Hertrich, M., 2008, Imaging of groundwater with nuclear magnetic resonance: Progress in Nuclear Magnetic Resonance Spectroscopy, **53**, 227–248, doi: 10.1016/j.pnmrs.2008.01.002.

Kenyon, W. E., J. J. Howard, A. Sezgine, C. Straley, A. Matteson, K. Horkowitz, and R. Ehrlich, 1989, Pore-size distriubtuion and NMR in microporous cherty sandstones: 13th Annual Logging Symposium, Society of Professional Well Log Analysts, Paper LL.

Legchenko, A., and O. A. Shushakov, 1998, Inversion of surface NMR data: Geophysics, **63**, 75–84, doi: 10.1190/1.1444329.

Legchenko, A., and P. Valla, 2002, A review of the basic principles for proton magnetic resonance sounding measurements: Journal of Applied Geophysics, **50**, 3–19, doi: 10.1016/S0926-9851(02)00127-1.

Mohnke, O., and U. Yaramanci, 2005, Forward modeling and inversion of MRS relaxation signals using multi-exponential decomposition: Near Surface Geophysics, **3**, 165–185.

Mueller-Petke, M., and U. Yaramanci, 2010, QT inversion — Comprehensive use of the complete SNMR dataset: Geophysics, **75**, no. 4, W199–209, doi: 10.1190/1.3471523.

Seevers, D. O., 1966, A nuclear magnetic method for determining the permeability of sandstones: 33rd Annual Logging Symposium, Society of Professional Well Log Analysts, Transactions, Paper L.

Sukstanskii, A. L., and D. A. Yablonskiy, 2001, Theory of FID NMR signal dephasing induced by mesoscopic magnetic field inhomogeneities in biological systems: Journal of Magnetic Resonance, **151**, 107–117, doi: 10.1006/jmre.2001.2363.

Timur, A., 1969, Pulsed nuclear magnetic resonance studies of porosity, movable fluid, and permeability of sandstone: Journal of Petroleum Technology, **21**, 755–786, doi: 10.2118/2045-PA.

Walbrecker, J. O., M. Hertrich, and A. G. Green, 2009, Accounting for relaxation processes during the pulse in surface NMR data: Geophysics, **74**, no. 6 G27–G34, doi: 10.1190/1.3238366.

Walsh, D. O., 2008, Multi-channel surface NMR instrumentation and software for 1D/2D groundwater investigations: Journal of Applied Geophysics, **66**, 140–150, doi: 10.1016/j.jappgeo.2008.03.006.

Walsh, D. O., E. Grunewald, P. Turner, A. Hinnell, and P. Ferre, 2011, Practical limitations and applications of short dead time surface NMR: Near Surface Geophysics, **9**, 103–111.